NUMERICAL SIMULATIONS OF HEATING ANOMALY EFFECTS OF TIBETAN PLATEAU ON CIRCULATION IN SUMMER

Qian Yongfu (钱永甫), *Liu Xiaodong* (刘晓东)* and *Zhong Zhong* (钟 中)* *

Department of Atmospheric Sciences, Nanjing University, Nanjing

Received March 30, 1991

ABSTRACT

A 5-layer numerical model with $p-\sigma$ incorporated coordinate system and primitive equations is used to simulate the effects of heating anomaly at and over the Tibetan (Qinghai-Xizang) Plateau on the circulations in East Asia in summer. The model is described briefly in the text and the results are analysed in somewhat detail. Results show that the surface albedo, the drag coefficient, the evaporation rate and the ground temperature all have large influences on the circulation near the Plateau and in East Asia. When the heating at the surface increases, the Tibetan high in the upper troposphere intensifies, too. Its area enlarges and its axis tilts to northwest. The upper tropical easterly increase and shifts to north. The southwesterly in the lower troposphere, in consistence, also increases. The cross-equatorial low-level currents along Somali and South India are influenced to increase their speeds while those over North Australia decrease. The land low over the Asian Continent deepens. Meanwhile the upward motions over the land of east China and over the Indo-China Peninsula intensify and therefore the precipitation over those areas increases. However, along the coastal area of China the upward motions and therefore the precipitation decrease.

Atmospheric heat source anomaly has large influence on the circulation, too. Simulated results indicate that heat source anomaly in the lower atmosphere over the Plateau influences the intensity and the position of the monsoon circulation while that in the upper atmosphere only affects the intensity. The heating status over the Plateau has slight influence on the westerly jet, north of the Plateau, while it has strong effect on the subtropical jet at the mid and low latitudes.

Key words: heating effects of the Tibetan Plateau, numerical simulation of general circulation, effects of heating anomalies on circulation, effects of underlying surfaces

I. INTRODUCTION

The area of Tibetan Plateau is about 2.5×10^6 km^2 and its mean height is 4000 above sea level. It is the largest and highest plateau with the most complex topography in the world. As a large convex barrier extending to the mid troposphere, the Tibetan Plateau has special dynamic and thermodynamic effects on the atmospheric motions. A most evident property of the heating effect of the Tibetan Plateau is that its heating directly exerts on the mid troposphere when compared with other surface heatings. The position of the Plateau heat source happens to locate over the transitional zone of the seasonal subtropical westerlies and easterlies.

The heat source of the Tibetan Plateau can be divided roughly into two kinds, i.e. the

* Present affiliation: Lanzhou Institute of Atmospheric Physics, Academia Sinica, Lanzhou.

* * Present affiliation: Institute of Meteorology, PLA Air Force, Nanjing.

surface heat source and the air heat source. The former means the sensible and the latent heat fluxes into the atmosphere from the underlying ground or water surface, and the latter is the latent heat released in the atmosphere due to large scale or convective scale condensation. Because of the influence of clouds, the air heat source may be induced by long wave radiation. The intensity of the surface heat source mainly depends on the physical properties of the underlying surface, such as albedo, drag coefficient and moisture, meanwhile, it also depends on the heat storage in the soil. There have been a lot of studies on both the surface and the air heat sources and their influences on atmospheric circulations in the East Asia (Xu et al., 1985; Chen et al., 1981; Huang, 1981; Luo et al., 1984; Kuo and Qian, 1981; He et al., 1984; Shen et al., 1987), however, there have also been some debates about them. Especially the problem of what will be the response when heat source anomalies appear requests more studies. In this paper the authors used a modified version of the p–σ incorporated coordinate system primitive equation model with five atmospheric layers and one soil or water layer to conduct two groups of numerical experiments on the effects of heat source anomalies, in order to understand the responses of the atmosphere to the anomalies. The second paragraph of this paper briefly introduces the numerical model, the third one is written for the schemes of experiments, the fourth is devoted to the analyses and discussions of the results and some preliminary conclusions obtained in the experiments will be presented in the last paragraph.

II. BRIEF INTRODUCTION OF THE MODEL

The model adopts p–σ incoporated coordinate system in the vertical direction and the 400 hPa level is taken as the interface above which the pressure coordinate is used and below σ coordinate is used. The atmosphere is divided into 5 layers, two of them in the P coordinate system and others in σ system, the lowest layer is considered as the boundary layer with a constant pressure thickness of 50 hPa.

In order to take into account the land–air and the air–sea interactions the model includes a 40 cm thick soil layer and a 100 cm water layer as the sixth layer in the ground and in the water, respectively. The water layer is assumed at rest with no dynamic process.

The sketch of the model is shown in Fig. 1.

The governing equations in the σ system are as follows in general forms:

$$\frac{du}{dt} = -PG_x + f v + F_u \,, \tag{1}$$

$$\frac{dv}{dt} = -PG_y - f u + F_v \,, \tag{2}$$

$$\frac{dT}{dt} = \frac{\omega + \varepsilon}{C_p \rho} + F_T \,, \tag{3}$$

$$\frac{dq}{dt} = E - C + F_q \,, \tag{4}$$

$$\frac{\partial P_s^*}{\partial t} = -\nabla \cdot P_s^* V - \frac{\partial P_s^* \dot{\sigma}}{\partial \sigma} \,, \tag{5}$$

$$\frac{\partial \varphi}{\partial \sigma} = -\frac{RT}{\sigma + \dfrac{P_c}{P_s^*}} \,, \tag{6}$$

where

$$\frac{d}{dt} = \frac{\partial}{\partial t} + V \cdot \nabla + \dot{\sigma}\frac{\partial}{\partial \sigma} , \tag{7}$$

PG_x and PG_y are the pressure gradient components along x and y directions, respectively, ε the heating rate per volume, E and C the changing rates of the mixing ratio q, respectively, due to evaporation and condensation, F terms the rates of corresponding quantities owing to friction or eddy diffusion, the other notations are conventional.

The predictive equation for the mean temperature T_G in soil or water layer is

$$\frac{\partial T_G}{\partial t} = \lambda_e (T_S - T_G) , \tag{8}$$

where T_s is the surface temperature of ground or water computed from the heat balance equation at the surface. The value of λ_e depends on the surface properties, in the model λ_e is taken as equal to 4.0×10^{-4} s^{-1} over water and 3.5×10^{-6} s^{-1} in land.

There are quite complete physical processes in the model, for instance, solar radiation and longwave radiation, large–scale and convective–scale condensations, interactions of land–air and air–sea, horizontal and vertical eddy diffusions and so on. The details of the model physics can refer to papers published by Qian et al. (1985; 1988; 1988).

The latitude–longitude horizontal grid system is used in the model with grid size being $5° \times 5°$, time step is 15 min., the model topography is sketched in Fig. 2.

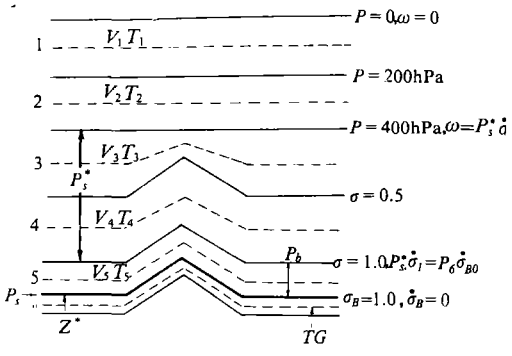

Fig. 1. Vertical structure of the model.

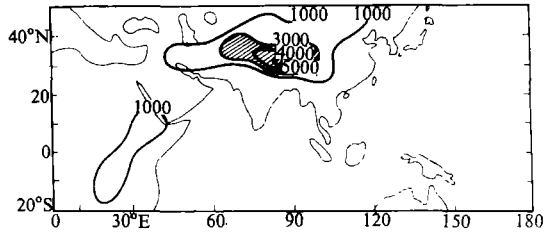

Fig. 2. Model topography (unit: 1m).

III. EXPERIMENTAL SCHEMES

As stated in the introduction two groups of experiments are conducted. The first group is designed for studying the responses of the atmospheric circulation to the heat source anomalies at the surface, therefore, the capital letter S is used to designate the group. The purpose of the second group is to study the response to the air heat source anomalies, designated by letter A.

1. *Experiments on the Surface Heat Source Anomalies (S)*

In S experiments, we put the focus on the influences of the underlying surface properties, there are following experiments:

(1) *Control experiment (SCTN)*

In SCTN, the surface albedo from Hummel's $10° \times 10°$ mean grid data (Hummel, 1979) is used after time and space interpolations, Fig. 3 is the distribution of the surface albedo.

(2) *Experiment of albedo change (SALB)*

The surface albedo given by Hummel are somewhat higher in the Tibetan Plateau area while lower in the desert area compared with some observations. Therefore, in SALB, we use modified value of albedos shown in Fig. 4.

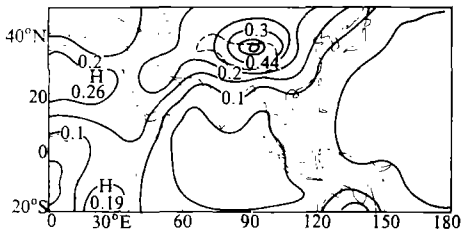

Fig. 3. Albedo in SCTN.

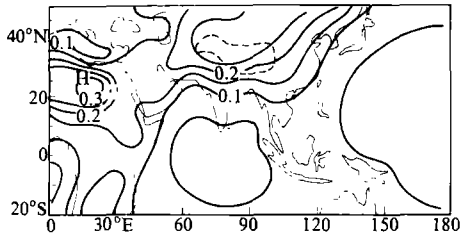

Fig. 4. Albedo in SALB.

(3) *Experiment on C_D change (SCDH)*

In SCDH, the drag coefficients over the Plateau surface higher than 3000 m are replaced by the observational data which are computed as the late June average C_D from the experiment conducted in May to August, 1979 (QXPMEX). As a result, the C_D value at each grid point is averagely enhanced by 0.0017.

(4) *Evaporation experiment (SEVH)*

In the control experiment (SCTN) the moisture at surface higher than 3000 m was taken as 0.1 of the saturation value, in SEVH it is on an average assumed 0.25. However, in the west part it changes very litte, the main enhancement is in the southeast part of the Plateau.

(5) *Negative T_G anomaly experiment (STGL)*

In STGL, the initial values of T_G in the soil at the points higher than 3000 m are set to be 2°C lower than the grid point mean values of T_G from the 6th to the 10th days in SCTN. Values at other points are still calculated from the model equation (8).

(6) *Positive T_G anomaly experiment (STGH)*

The experimental scheme is the same as STGL, except that in STGH the T_G initial values are set to be 2° higher.

(7) *Composite experiment (STOT)*

In this experiment, the surface albedo, C_D and mean soil temperature T_G are given according to the corresponding experiments SALB, SCDH and STGH, respectively.

2. *Experiments on the Air Heat Source Anomalies (A)*

In group A of experiments, the June monthly zonally averaged temperature and geopotential height fields were taken as the initial fields of the model. After 20–day integration, a near equilibrium state was obtained which basically represents the summer mean pattern of

the circulation and the mean air heat sources. Then the pattern was input as the initial state of the experiments. Let the mean air heat source field be fixed, and integrate the model to another 5 days, we can get a state which is taken as the control run and designated as ACTN. By using the same initial condition and increasing or decreasing the heating rates at the grid points higher than 3000 m in the first and the fifth layers, respectively, by 1K / d and 2K / d, we get 4 experimental results after 5–day integration and designate them by AHI, AHD, ALI and ALD, respectively, they can be compared with the ACTN. Table 1 shows the main indexes, where the column of heating rate change gives the absolute and the relative values (in parentheses). It is seen from the table that the absolute value of heating rate change is larger in the iower layer than that in the upper layer, however, for the relative value which is the ratio of the absolute value to the mean heating rate of the area, the case is reverse.

Table 1. Main Indexes of Air Heat Source Anomalies

Experiment notation	Experimental schemes	Heating rate change	Location of heating rate change
ACTN	Normal		
ALI	+	2K / d(1 / 8)	fifth model layer
ALD	−	−2K / d(−1 / 8)	fifth model layer
AHI	+	1K / d(1 / 2)	first model layer
AHD	−	−1K / d(−1 / 2)	first model layer

Note: +denotes positive anomaly; − negative anomaly.

In both groups of the experiments the model domain is limited in 25°S—55°N, 0—180°E, which is the most evident monsoon region, therefore, most evidently influenced by the Tibetan Plateau. The boundary conditions in group S are set to allow changing from the initial state to the climatic one finally, while those in group A are set fixed during integration.

IV. ANALYSES AND DISCUSSIONS OF THE EXPERIMENTAL RESULTS

There are a good many of experimental results obtained from the simulations, such as geopotential height, temperature, horizontal and vertical flow, heat source and precipitation (in group S) fields and so on. However, in order to save space and time we are going to analyze, discuss and compare the most important ones in this paragraph which can reveal the largest differences between each other of the experiments.

1. *Analysis and Discussion of Group S*

(1) *SCTN experiment*

Some simulated results are given in SCTN in order to show the ability of the model to reproduce the climatic mean patterns of the summer Northern Hemisphere.

Figs.5a, b and c are the simulated 200 hPa flow pattern (a), the meridional circulations along 90°E at the daytime (b) and nighttime (c).

From Fig. 5 it is seen that there is an anticyclonic centre at 27.5°N and 95°E at the 200 hPa level which fairly agrees with observations. Over the main part of the Tibetan Plateau along 90°E there is a strong vertical monsoon cell, south of 20°N, either at daytime or at the nighttime. Above the Plateau and its vicinity the upward motion dominates at daytime while downward motion at nighttime, it shows the evident diurnal variation in flow field and consequently that in

heating field in the Plateau region.

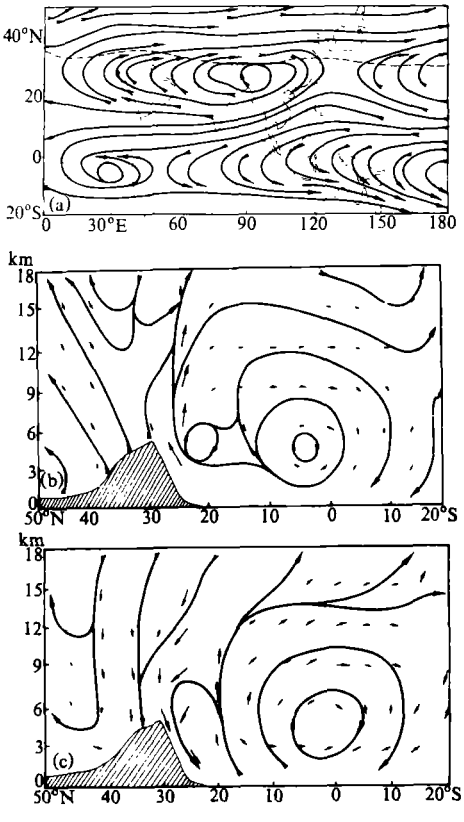

Fig. 5. Simulated results in SCTN. (a) 200 hPa flow pattern, (b) daytime mean meridional circulation, and (c) nighttime mean meridional circulation.

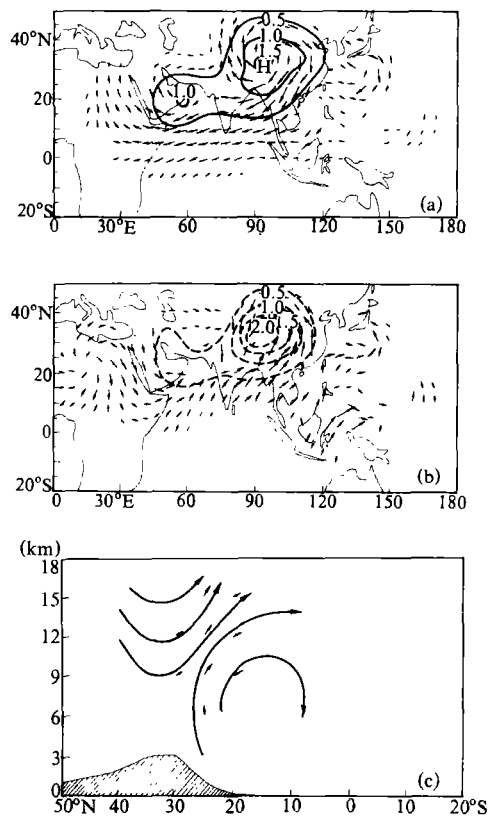

Fig. 6. Differences of SALB from SCTN. (a) 200 hPa differential wind vectors, (b) differential wind vectors in boundary layer, and (c) differential meridional circulation along 90°. Isolines are isanemone in m / s.

(2) *SALB experiment*

The reduction in the Plateau area and the enhancement in the desert area of the surface albedo in SALB make the heating effect increase in the former and decrease in the latter, therefore, influence the circulation patterns. Figs. 6a and b are the differences of wind vectors at the 200 hPa level and in the boundary layer, respectively, in the SALB from those in the SCTN. We can see that the anticyclone at the upper level strengthens, the Tibetan high increases its height and enlarges, the centre of the high moves northward in comparison with that in Fig.5a. In the boundary layer the Tibetan low deepens, therefore, the southerly component of the flow increases, a cyclonic circulation of the differential vector field over the sea surface south of Japan offsets the anticyclonic flow, consequently decreases the western Pacific high existing originally in that area. It is worthy to indicate that differential northerly component appears over the equa-

torial western Pacific which weakens the flow across the equator there. From above analysis it is seen that the heat source anomaly over the Tibetan Plateau has opposite effects on the Somali jet, the Indian south westerly and the East Asian cross–equatorial air current. Besides, a differential anticyclonic circulation appears over the Sahara desert and weakens the heat low there.

The reduction of the Plateau surface albedo increases the strength of the vertical monsoon circulation along 90°E. Fig. 6c is the differential meridional profile between the two experiments. The most important influence of the Plateau heat source anomaly is on the upward motion along the south slope of the Plateau, hence, also on the precipitation intensity there.

(3) *STGH and STGL experiments*

In those two experiments the Plateau surface heat source increases and decreases, respectively. It can be imaged that in STGH the simulated results should be similar to those in SALB, i.e. the Tibetan high in the upper atmosphere and the Tibetan heat low are both intensified. In STGL, the case should be reverse. Therefore, the comparison of the two experiments can reveal the influences of the soil temperature anomaly in the Plateau area on the circulations more evidently.

Figs. 7a and b are the differential wind vectors of the two experiments at the 200 hPa level and in the boundary layer, respectively. The figures show that the upper–level high and the lower–level low over the Plateau have large differences in intensity because of the positive and negative anomalies of the soil temperature. The maximum speed difference at the upper level is about 1.5 m / s and that at the low level is about 2.5 m / s. Figs. 7a and b are quite similiar to Figs. 6a and b in the Plateau area, although the main influence of the soil temperature anomaly is located in the Plateau area and its vicinity, the effect can expand to the whole Asian continent.

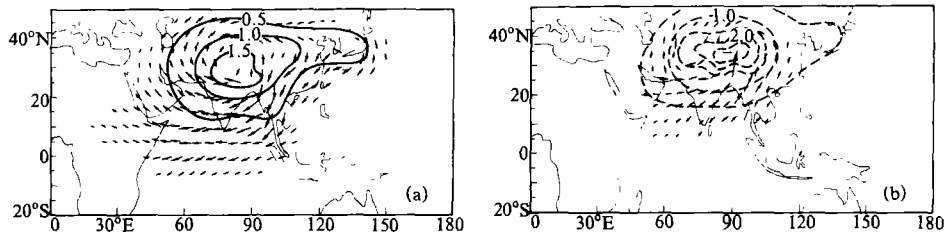

Fig. 7. Differential wind vectors of STGH from STGL (a) at 200 hPa, and (b) in boundary layer.

(4) *SCDH and SEVH experiments*

The increase of the drag coefficient C_D over the Plateau means that the exchanges of heat, moisture and momentum fluxes between ground surface and the air are enhanced, therefore, when the Plateau ground surface is heated, the sensible heat from the ground to the air is increased, at the nighttime, the ground surface is cooled, the sensible heat is transferred from the air to the ground, those two tendencies seem to offset each other. However, in summer the daytime is longer than the nighttime, the increase of C_D is still able to affect the circulation features. The simulated results prove that the increase of C_D can somewhat enhance the 200 hPa level high, but not as evidently as in SALB. An interesting fact is that the lower level circulation

is very little influenced by the C_D increase, and some responses are even opposite to those in SALB.

The increased evaporation increases the moisture transfer from the ground to the air and therefore also increases the potential precipitation due to possible condensations in the upper atmosphere. The latent heat released can heat the upper level air and influence the atmospheric motions, however, the lower atmospheric circulation is influenced a little.

(5) *STOT experiment*

As stated in the preceding paragraph, in the STOT the albedo decreases, the C_D increases and the positive anomaly of the soil temperature T_G exists at the grid points higher than 3000 m over the Tibetan Plateau, therefore, the heating effect of the Plateau is largely enhanced. Reversely, the heating effect in STGL is weakened. Hence the comparison of STOT with STGL is more evident to show the influences of the surface heat source anomalies on the atmospheric circulations.

Figs. 8a and b are the differences of STOT from STGL in the 200 hPa level geopotential field and in the sea-level surface pressure field, respectively. From the figures it is seen that the Tibetan high in STOT is much stronger than in STGL, the maximum difference of geopotential heights is 3.35 decametres, furthermore, the positive deviation occupies almost the whole domain of integration except for the Indian Ocean where exist small negative deviations. The land heat low largely deepens, the difference at the low centre is about 4 hPa and the domain where changes take place is the same as that of the upper level high, they match very well. Therefore, from the pressure patterns the heating anomaly of the Plateau evidently influences a pair of semi-permanent climatic systems in the upper and the lower atmosphere over the Plateau.

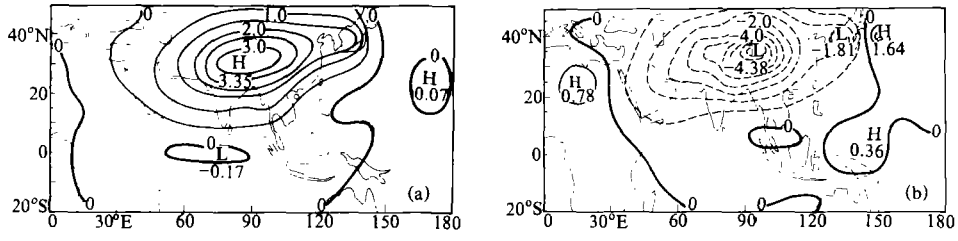

Fig. 8. Pattern differences of STOT from STGL (a) at 200 hPa; and (b) at sea-level surface.

The pattern differences in the geopotential and the pressure field are the reflections of those in the heating fields. Figs. 9a, b and c are the differential mean heating rates (in K / d) between STOT and STGL along 75—85°E (a), 95—105°E (b) and 105—120°E (c), respectively. Each of them represents the situation of the west part, the east part of the Plateau and the east region of the Asia. From Fig. 9, we see that the positive deviations in the west part appear at the upper level over 35°N and extend vertically to the 12 km level, above which and over 20°N there are negative deviations. The maximum heating rate difference is 3.23K / d and exists at the 5 km level, which is no doubt induced by the enhanced sensible heat flux, the negative area over 20°N and above 12 km results from the longwave radiation cooling. Over the east part of the Plateau, the positive differences are of appearance at 9 km level over 25°N, above 12 km and south of 20°N there are weak negative deviations. It seems that the positive centre may be induced by the increasing latent heating. The maximum reaches 4.37K / d which is larger than that over the

west part. Over the East Asian area, there is a centre of positive difference with 1.88K / d at the 9 km level, 35°N, which is also considered as a result of latent heat increase, in the surroundings there is a wide negative area.

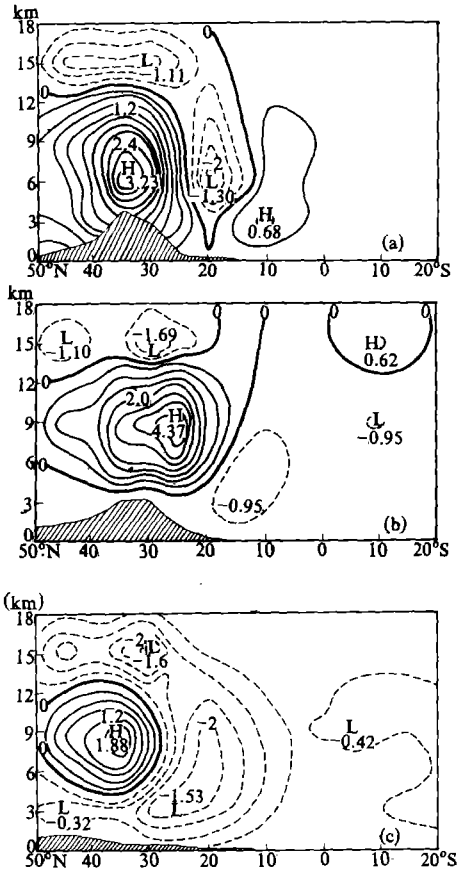

Fig. 9. Differential heating rates of STOT from STGL, averaged along 75—85°E (a), 95—105°E (b) and 105—120°E (c), unit: K / d.

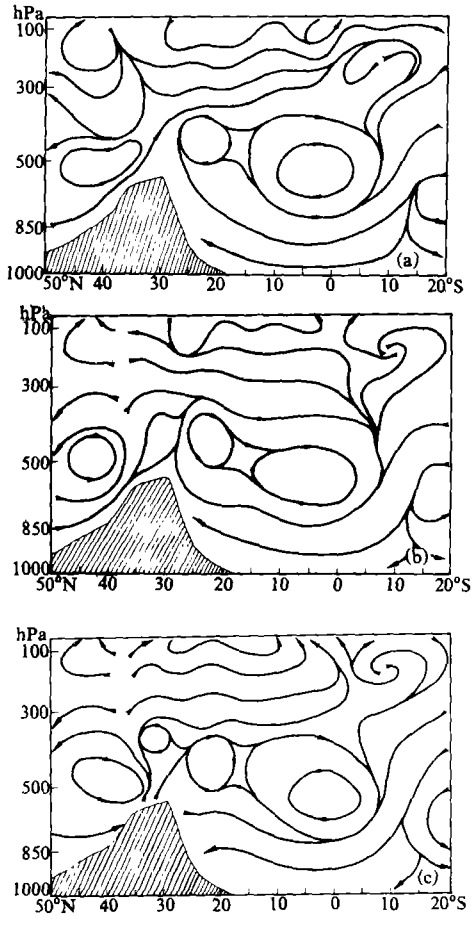

Fig. 10. Meridional circulation along 90°E in (a) ACTN, (b) ALI. and (c) ALD.

It is not difficult to see from above analysis that the mechanism of the heating anomaly over the Plateau may be different in various regions. The same surface heat source anomaly functions in the west part as sensible heat, while in the east functions through latent heat release. Meanwhile the latent heat anomaly over the east Plateau is quantitatively larger than that over both the west Plateau and East Asia.

Further analysis of the mean zonal flows along meridional profiles and the vertical motions and precipitations also indicates that the heat anomaly of the Plateau can influence the wide area of the integration, therefore, it is indeed a very important factor for the East Asian circulation and climate.

2. *Analysis and Discussion of Group A*

(1) *ACTN experiment*

As the control test, the simulated results are quite similar to those in SCTN, though the two groups have different initial states and different lateral boundary conditions. The similarity means that the model has fairly good capability of modelling and the East Asian circulation patterns are mainly dependent upon the heating effects of the Tibetan Plateau.

Fig. 10a is the meridional circulation of ACTN along 90°E. From the shape and the position of the monsoon cell we can see that they are similar to that in SCTN (Fig. 5b), the only difference is that the upward motion south to the Plateau is a little weaker and there exist northerly components north to the Plateau. The pressure patterns in the upper and the lower atmosphere are similar, too. We will not give further discussions here in order to save space.

(2) *ALI and ALD experiments*

In those experiments the heating rates in the boundary layer are increased and decreased by 2K / d, respectively, Figs. 10b and c are the meridional circulations along 90°E in ALI and ALD. Compared with that in Fig. 10, they are seen very similar. However, in ALI the cell north to the Plateau develops better because of the increased heating rates in the Plateau boundary layer and consequently of the increased upward motions there. In ALD, the heating rates are reduced, a small cell right over the Plateau appears, that means the upward motions decrease and the downward motions increase. From Figs. 10b and c, it is also seen that the effects of heating rate anomalies in the Plateau boundary layer are mainly limited to the Plateau and its vicinity.

(3) *AHI and AHD experiments*

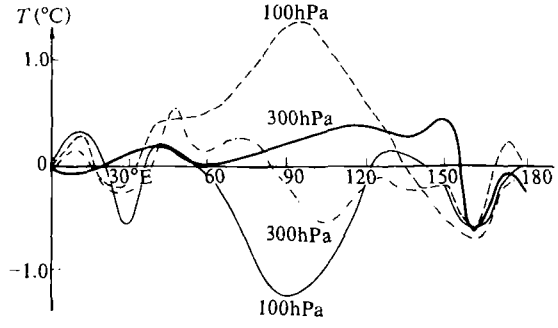

Fig. 11. Longitudinal distributions of temperature deviations in AHI (dotted curves) and AHD (solid curves) from ACTN along 35°N at 100 hPa and 300 hPa levels.

In AHI and AHD the heating rates at the 100 hPa level are increased and decreased by 1 K / d, respectively. Fig. 11 shows the longitudinal distributions of the temperature deviations of the two experiments from ACTN along 35°N at the 100 and 300 hPa levels. It is seen that the 100 hPa temperatures over the Plateau area are higher in AHI than in ACTN, while the 300 hPa temperatures are higher in the west Plateau and lower in the east Plateau. When the 100 hPa heating rates decrease (in AHD), the case is just reverse. An interesting thing is that in both experiments there are negative differences in temperature field near 30°E and 160°E.

Figs. 12a, b are the meridional profiles along 90°E (a) and 120°E (b), respectively, of the differential zonal components in AHI from ACTN. It is shown that the air heat source anomaly is located in the upper atmosphere, the easterly components south to the Plateau increase along 90°E, while south to 15°N the westerly components increase down to the equator, the zonal components just over and north to the Plateau are affected to a very little extent. Along 120°E the zonal components either at the high level or at the low level are largely influenced in the tropical and subtropical regions, while they are little affected in the mid and high latitudes.

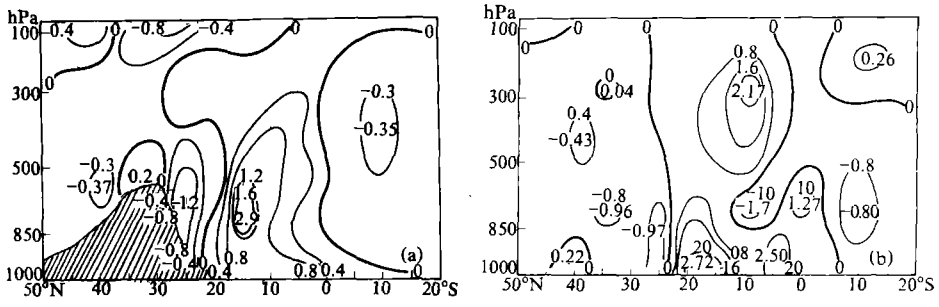

Fig. 12. Differential zonal components along 90°E (a) and 120°E (b) in AHI from ACTN (m / s).

In AHD the case is similar but with opposite signs. Talking about the influences of the upper air heat anomaly on the monsoon circulation the main function is to change the intensities of the upward and the downward motions, its shape changes very little.

V. SOME CONCLUSIONS

Through the above analyses and discussions of the two groups of numerical experiments, we can roughly obtain the following primary conclusions:

(1) Changes in the surface properties and thermal status of the Tibetan Plateau have evident influences on the East Asian circulation and the southern Asian monsoon. When the surface heat source increases, the upper–level Tibetan high and its anticyclonic flow intensify, the area enlarges, the main body of the high shifts to northwest, the tropical easterly south to the high strengthens with its position northward. North to the Plateau the northerly wind components increase and the southwesterly monsoon along India, the Somali jet across the equator and the southerly wind north to Australia are all enhanced, while the differential northerly exists over Indonesia in the boundary layer, which increases the convergence there.

(2) The positive heat source anomaly on the Plateau surface increases the upward motions and, consequently, the precipitation amount over the Indo–China Peninsula and Changjiang–Weihe valleys of China. The rainfall amount over the Plateau itself and the mid of India does not increase evidently. Reversely the upward motion and precipitation over the east coastal area of China decrease.

(3) When the Plateau surface heat source increases, the heating field in the atmosphere increases as well. The atmospheric heat sources over the Plateau, especially over the northeast part of the Bay of Bengal, evidently intensify. The enhancement of heat sources over the west part, the east part of the Plateau and East Asia may result from the different mechanisms.

(4) The heat source anomaly in the air has large effects on the circulations, too. The

low-level air heat source anomaly results in the changes of the intensity and the position of the South Asian monsoon circulation, while the upper-level air heat source anomaly only changes its intensity. The heat anomaly over the Plateau has less influence on the westerly jet while large influence on the zonal wind components in the mid and low latitudes.

Above are the preliminary results. More studies are needed, especially studies on the relations between heat source anomalies and the extents to which the anomalies influence the circulations.

REFERENCES

Chen Longxun, Li Weiliang and He Jiahua (1982), On the atmospheric heat source over Asia and its relation to the formation of the summer circulation, *Mountain Meteorology*, pp.265—290, Science Press, Beijing (in Chinese).

Chen Qigong et al. (1981), The relations between mean temperature distribution over Tibetan Plateau and early summer drought and flood in the mid and low reaches of Changjiang River, *Collected Papers on Tibetan Plateau Meteorology*, Science Press, Beijing (in Chinese).

He Jiahua et al. (1984), Preliminary results of numerical modellings of the effects of atmospheric heat sources and Tibetan Plateau on monsoon circulations, *Papers on QXPMEX* (I), pp.324— 329, Science Press, Beijing (in Chinese).

Huang Zhongyuan (1981), Relations between Tibetan Plateau thermal states and drought-flood in Changjiang River valley, *Collected Papers on Tibetan Plateau Meteorology*, Science Press (in Chinese).

Hummel and Reck, (1979), A global surface albedo model, *J. Appl. Met.*, **18**:239—253.

Kuo, H. L. and Qian, Y. (1981), Influence of Tibetan Plateau on cumulative and diurnal changes of weather and climate in summer, *Mon. Wea. Rev.*, **109**: 2337—2356.

Luo Siwei et al.(1984), Seasonal transfer from summer to autumn in the Tibetan Plateau area, *Papers on QXPMEX* (I), pp.193—202, Science Press (in Chinese).

Qian Yongfu (1985), A five-layer primitive equation model with topography, *Plateau Meteorology*, **4(2)**:1—28 (in Chinese).

Qian Yongfu, Yan Hong, Wang Qianqian and Wang Anyu (1988), *Numerical Studies on Topographic Effects in the Planetary Atmosphere*, Science Press (in Chinese).

Qian Yongfu (1988), A scheme of calculation of heat balance temperature at ground surface, *Scientia Meteorologica Sinica*, **No.4: 14—27 (in Chinese).**

Shen Rujin et al. (1987), Numerical experiments of the thermal effects of Tibetan Plateau, *Papers on QXPMEX* (III), Science Press (in Chinese).

Xu Guochang and Li Meifang (1985), The relationship between Qinghai-Xizang Plateau and the circulation over East Asia, *Plateau Meteorology*, **4**:185—189 (in Chinese).

Zhen, Q. and Liou, K-N (1986), Dynamic and thermodynamic influence of the Tibetan Plateau on the atmosphere in a general circulation model, *J. Atmos. Sci.*, **43**:1340—1354.